# Storing Freshwater Versus Storing Electricity in Power Systems with High Freshwater Electric Demand

Mubarak J. Al-Mubarak, *Graduate Student Member*, *IEEE*, and Antonio J. Conejo, *Fellow*, *IEEE*

*Abstract*—We consider a power system whose electric demand pertaining to freshwater production is high (high freshwater electric demand), as in the Middle East, and investigate the tradeoff of storing freshwater in tanks versus storing electricity in batteries at the day-ahead operation stage. Both storing freshwater and storing electricity increase the actual electric demand at valley hours and decrease it at peak hours, which is generally beneficial in term of cost and reliability. But, to what extent? We analyze this question considering three power systems with different generation-mix configurations, i. e., a thermal-dominated mix, a renewable-dominated one, and a fully renewable one. These generation-mix configurations are inspired by how power systems may evolve in different countries in the Middle East. Renewable production uncertainty is compactly modeled using chance constraints. We draw conclusions on how both storage facilities (freshwater and electricity) complement each other to render an optimal operation of the power system.

*Index Terms*—Power system operation, freshwater production and transportation, coordination, day-ahead scheduling.

## NOMENCLATURE

### A. Power System

#### 1) Indices and Sets

| | |
|---|---|
| $\mathcal{A}_u$ | Feasibility set regarding minimum-up time and minimum-down time for gas unit $u$ |
| $\chi_r^{U}$ | Gas units in reliability region $r$ |
| $\Omega_n^{B}$ | Battery units at node $n$ |
| $\Omega_n^{K}$ | Wind units at node $n$ |
| $\Omega_n^{S}$ | Pumps at node $n$ |
| $\Omega_n^{U}$ | Gas units at node $n$ |
| $\Omega_n^{V}$ | Photovoltaic (PV) units at node $n$ |
| $\Omega_n^{Z}$ | Electric demands not related to freshwater production at node $n$ |
| $b$ | Batteries |
| $k$ | Wind units |
| $n, \ell$ | Electrical nodes and transmission lines |
| $r$ | Reliability regions |
| $r(\ell), s(\ell)$ | Receiving-end and sending-end nodes of line $\ell$ |
| $t$ | Hours |
| $u$ | Gas units |
| $v$ | PV units |
| $z$ | Electric demands not related to freshwater production |

#### 2) Parameters

| | |
|---|---|
| $\alpha_u^{E}$ | Production cost of gas unit $u$ ($/MWh) |
| $\alpha_u^{F}$ | No-load cost of gas unit $u$ ($/h) |
| $\alpha_z^{LS}$ | Load-shedding cost of electric demand $z$ ($/MWh) |
| $\alpha_v^{PV}$ | Operation cost of PV unit $v$ ($/MWh) |
| $\alpha_u^{SD}$ | Shut-down cost of gas unit $u$ ($/h) |
| $\alpha_u^{SU}$ | Start-up cost of gas unit $u$ ($/h) |
| $\alpha_k^{W}$ | Operation cost of wind unit $k$ ($/MWh) |
| $\phi_u^{U}, \phi_u^{D}$ | Ramp-up and ramp-down limits of gas unit $u$ (MW/h) |
| $\phi_u^{SU}, \phi_u^{SD}$ | Start-up and shut-down ramp limits of gas unit $u$ (MW/h) |
| $\eta_b^{C}, \eta_b^{D}$ | Charging and discharging efficiencies of battery $b$ (p.u.) |
| $\mu_{PV_v}(t)$ | Hourly average of forecast power output of PV unit $v$ (MW) |
| $\mu_{W_k}(t)$ | Hourly average of forecast power output of wind unit $k$ (MW) |
| $\sigma_{PV_v}(t)$ | Hourly standard deviation of power output of PV unit $v$ (MW) |
| $\sigma_{W_k}(t)$ | Hourly standard deviation of power output of wind unit $k$ (MW) |
| $1 - \epsilon$ | Security level |
| $\phi^{-1}(\cdot)$ | Inverse cumulative distribution function of standard normal distribution |
| $E_b^{\max}$ | Energy capacity of battery $b$ (MWh) |

| $E_b^{\min}$ | The minimum energy content of battery $b$ (MWh) |
|---|---|
| $F_\ell^{\max}$ | Capacity of line $\ell$ (MW) |
| $K_\ell$ | Susceptance of line $\ell$ (S) |
| $P_b^{\mathrm{Ch,max}}$ | Charging capacity of battery $b$ (MW) |
| $P_b^{\mathrm{Dis,max}}$ | Discharging capacity of battery $b$ (MW) |
| $P_u^{\mathrm{E,min}}$ | The minimum power output of gas unit $u$ (MW) |
| $P_u^{\mathrm{E,max}}$ | Capacity of gas unit $u$ (MW) |
| $P_z^{\mathrm{ZE}}(t)$ | Load of electric demand $z$ during hour $t$ (MW) |
| $R_r(t)$ | Reserve requirement in region $r$ during hour $t$ (MW) |
| $T$ | Total time (hour) |

*3) Variables*

| $\theta_n(t)$ | Voltage angle of node $n$ during hour $t$ (rad) |
|---|---|
| $E_b^{\mathrm{B}}(t)$ | State-of-charge (SOC) of battery $b$ at the end of hour $t$ (MWh) |
| $f_\ell^{\mathrm{E}}(t)$ | Power flow through line $\ell$ during hour $t$ (MW) |
| $P_b^{\mathrm{Ch}}(t)$ | Charging power to battery $b$ during hour $t$ (MW) |
| $P_b^{\mathrm{Dis}}(t)$ | Discharging power from battery $b$ during hour $t$ (MW) |
| $P_u^{\mathrm{E}}(t)$ | Power output of gas unit $u$ during hour $t$ (MW) |
| $\bar{P}_u^{\mathrm{E}}(t)$ | The maximum power output of gas unit $u$ during hour $t$ (MW) |
| $P_z^{\mathrm{LS}}(t)$ | Load shed from electric demand $z$ during hour $t$ (MW) |
| $P_v^{\mathrm{PV}}(t)$ | Power output of PV unit $v$ during hour $t$ (MW) |
| $P_k^{\mathrm{W}}(t)$ | Power output of wind unit $k$ during hour $t$ (MW) |
| $w_u(t)$ | 0-1 variable (equal to 1 if gas unit $u$ is on, and 0 otherwise) |
| $x_u(t)$ | 0-1 variable (equal to 1 if gas unit $u$ is shut down at the beginning of hour $t$, and 0 otherwise) |
| $y_u(t)$ | 0-1 variable (equal to 1 if gas unit $u$ is started up at the beginning of hour $t$, and 0 otherwise) |

**B. Freshwater System**

*1) Indices and Sets*

| $\mathcal{D}_c$ | Feasibility set regarding freshwater production for desalination plant $c$ |
|---|---|
| $\Omega_i^{\mathrm{C}}$ | Desalination plants at node $i$ |
| $\Omega_i^{\mathrm{M}}$ | Freshwater demands at node $i$ |
| $\Omega_i^{\mathrm{Q}}$ | Freshwater tanks at node $i$ |
| $c, i, j$ | Desalination plants, freshwater nodes, and pipelines |
| $j\{s\}$ | Pipeline $j$ associated with pump $s$ |
| $m, q, s$ | Freshwater demands, freshwater tanks, and pumps |
| $r(j), s(j)$ | Receiving-end and sending-end nodes of pipeline $j$ |

*2) Parameters*

| $\alpha_m^{\mathrm{UW}}$ | Unserved-freshwater cost of demand $m$ ($/m$^3$) |
|---|---|

| $\mu_s, \beta_s$ | Performance parameters of pump $s$ (p.u.) |
|---|---|
| $\eta_s$ | Efficiency of pump $s$ (p.u.) |
| $\lambda$ | Unit weight of freshwater (N/m$^3$) |
| $d_m^{\mathrm{W}}(t)$ | Freshwater requirement of demand $m$ during hour $t$ (m$^3$/h) |
| $f_q^{\mathrm{C,max}}$ | The maximum inflow to freshwater tank $q$ (m$^3$/h) |
| $f_q^{\mathrm{D,max}}$ | The maximum outflow from freshwater tank $q$ (m$^3$/h) |
| $f_j^{\mathrm{W,max}}$ | Capacity of pipeline $j$ (m$^3$/h) |
| $g_c^{\mathrm{W,max}}$ | Freshwater capacity of desalination plant $c$ (m$^3$/h) |
| $h_i^{\mathrm{P,min}}$ | The minimum pressure head of freshwater at node $i$ (m) |
| $h_i^{\mathrm{P,max}}$ | The maximum pressure head of freshwater at node $i$ (m) |
| $h_i^{\mathrm{Z}}$ | Elevation head of freshwater at node $i$ (m) |
| $P_s^{\mathrm{WP,max}}$ | Capacity of pump $s$ (MW) |
| $R_j$ | Resistance of pipeline $j$ |
| $V_q^{\mathrm{W,max}}$ | Capacity of tank $q$ (m$^3$) |
| $V_q^{\mathrm{W,min}}$ | The minimum freshwater volume of tank $q$ (m$^3$) |

*3) Variables*

| $\omega_s^{\mathrm{WP}}(t)$ | Relative angular speed of pump $s$ (p.u.) |
|---|---|
| $d_m^{\mathrm{UW}}(t)$ | Unserved freshwater of demand $m$ during hour $t$ (m$^3$/h) |
| $f_q^{\mathrm{C}}(t)$ | Inflow to freshwater tank $q$ during hour $t$ (m$^3$/h) |
| $f_q^{\mathrm{D}}(t)$ | Outflow from freshwater tank $q$ during hour $t$ (m$^3$/h) |
| $f_j^{\mathrm{W}}(t)$ | Freshwater flow through pipeline $j$ during hour $t$ (m$^3$/h) |
| $g_c^{\mathrm{W}}(t)$ | Freshwater output of desalination plant $c$ during hour $t$ (m$^3$/h) |
| $h_s(t)$ | Head rise of freshwater by pump $s$ during hour $t$ (m) |
| $h_j^{\mathrm{F}}(t)$ | Friction loss of pipeline $j$ during hour $t$ (m) |
| $h_i^{\mathrm{P}}(t)$ | Pressure head of freshwater at node $i$ during hour $t$ (m) |
| $P_s^{\mathrm{WP}}(t)$ | Power demand of pump $s$ during hour $t$ (MW) |
| $V_q^{\mathrm{W}}(t)$ | Freshwater volume of tank $q$ at the end of hour $t$ (m$^3$) |

## I. Introduction

THE increasing demand for freshwater and the limited availability of freshwater resources in arid areas have resulted in the installation of an increasing number of desalination plants. This is the case in most countries in the Middle East, where desalination is the main source of freshwater. Specifically, each day, 48% of the 95000000 m$^3$ of desalinated freshwater produced globally is in the Middle East and North Africa [1]. We note that reverse osmosis (RO) is the prevailing technology for freshwater production and thus the most widely used in new programs and projects concern-

ing freshwater production. For instance, Kuwait has installed one RO plant in Az-Zour with a total capacity of 136600 $m^3$ per day and another RO plant in Doha with a total capacity of 272765 $m^3$ per day [2]. In addition, Al Taweelah station in Abu Dhabi currently produces 454609 $m^3$ per day. This production is expected to increase to 909218 $m^3$ per day in the near future [3].

In this paper, we consider a power system with high freshwater electric demand, that is, a power system whose electric demand pertaining to freshwater production is high (as in the Middle East), and investigate the tradeoff of storing freshwater in tanks versus storing electricity in batteries at the scheduling stage (one day in advance). We note that desalination plants consume almost solely electricity to produce freshwater out of salty water.

Freshwater storage shifts the electrical load by storing freshwater for later use and has the potential to do this at a massive and centralized scale. This process resembles thermal storage but at the bulk level: while thermal storage has generally a local and small-scale impact, freshwater storage at the bulk level has the potential to alter the scheduling and functioning of a power system that contains an important freshwater system.

Particularly, filling up freshwater tanks during hours of excess of electricity and reducing production level of freshwater during hours of high electric demand is beneficial economically and in terms of reliability. Similarly, charging batteries with excess electrical energy during hours when electric demand is low and discharging batteries during hours when electric demand is high lead to economic and reliability benefits. But, what is the best combination of storing freshwater in tanks versus storing electricity in batteries?

Although it is clear that building freshwater tanks is generally cheaper than installing electrical batteries, these two storage mechanisms complement each other. Our work seeks to point out and analyze this cross-effect. To study this cross-effect, we examine three power systems with different generation-mix configurations, i.e., a thermal-dominated mix, a renewable-dominated one, and a fully renewable one. These generation-mix configurations are inspired on how power systems may evolve in different countries in the Middle East.

Besides, renewable production uncertainty, which is the most important, is compactly modeled using chance constraints, which are transformed into deterministic conditions for computational simplicity [4].

We perform simulations using the IEEE 118-bus system [5] linked to two 13-node freshwater systems [6]. We extract conclusions on how both storage facilities (freshwater and electricity) complement each other to render an optimal day-ahead operation of the power system.

Reference [7] studies the day-ahead economic scheduling problem for a microgrid that incorporates thermal units, photovoltaic (PV) units, wind units, and batteries on the power system side, and hybrid electrodialysis-RO units, reservoirs, and freshwater tanks on the freshwater system side. A mixed-integer nonlinear programming problem is proposed to analyze the coordinated operation of the power-freshwater system. The study shows that the system operates at a lower

cost and a lower peak as a result of including tanks in the freshwater system and by using solely renewable units in the power system.

A day-ahead economic scheduling problem for power, gas, and freshwater systems, while considering wind power output uncertainties, is studied in [8]. A nonlinear but convex two-stage robust optimization model is developed, and Bender's decomposition is used to solve the resulting problem.

A power-freshwater system with uncertain renewable power production is studied in [9]. A data-driven method is used to model renewable uncertainties. Convex relaxation as well as piecewise linearization techniques is used to represent nonlinear freshwater system constraints. A mixed-integer linear model is developed for the day-ahead operation of the integrated system. Reference [9] shows that incorporating freshwater tanks in the coordinated model generally reduces the curtailed power and the peak demand.

A day-ahead scheduling problem for a power-freshwater system is considered in [10]. A mixed-integer linear model is proposed, which considers energy production and transmission constraints for the power system, and solely freshwater production constraints for the freshwater system. A coordinated operation without any batteries is compared with an operation that incorporates both freshwater tanks and batteries.

A mixed-integer nonlinear programming model for the operation of a distribution-level power-freshwater system is developed in [11]. Energy storage, pump operation, and pipeline loss constraints are approximated using convex hull and quasi-convex hull relaxations. With these approximations, the model becomes a mixed-integer quadratically constrained quadratic program. Flexible operation of freshwater tanks is considered to facilitate the optimal operation. However, a detailed desalination plant description is not considered in [11].

A mixed-integer nonlinear programming model for the joint power-freshwater system with wind production uncertainty is reported in [12]. A convex approximation is implemented to represent nonlinear pump operation constraints. A power-to-gas model is integrated in the power-freshwater system, and the day-ahead operation for the integrated system is considered.

In [13], a single-period optimal power and freshwater flow problem that considers the uncertainties of the demand and the production of renewable units is proposed and analyzed. The formulation considers a linear model for the power system and a nonlinear one for the freshwater system. A piecewise linearization technique is implemented on nonlinearities that renders a mixed-integer linear programming (MILP) model.

To the best of our knowledge, no study in the literature considers the day-ahead scheduling problem for a bulk power system (spanning a country or region) taking into account renewable uncertainties and including a detailed description of freshwater production and transportation. In this context, with the target of analyzing the tradeoff of storing freshwater in tanks versus storing electricity in batteries, we propose a model that includes detailed descriptions of the operation of the power system and the production and transportation of freshwater, and consider the uncertainties of PV and wind

units.

Considering the above literature review and the proposed model, the contributions of this paper are as follows.

1) An accurate mathematical description of a power system (at the bulk level) is provided with freshwater production and transportation constraints, while representing renewable uncertainties.

2) The impacts of increasing renewable penetration on the operation of the power system and the production of freshwater are studied.

3) The daily operation of freshwater tanks and electric batteries as the renewable penetration increases is specifically compared.

The remainder of this paper is organized as follows. Section II develops a model for the day-ahead scheduling of a power system with a detailed description of freshwater production and transportation. Section III investigates three case studies involving different renewable penetration levels and using the IEEE 118-bus system and two freshwater systems. Finally, Section IV provides conclusions.

## II. POWER-FRESHWATER SYSTEM FORMULATION

In this section, we formulate and characterize the power system considered: a power system that includes large electric demands pertaining to freshwater production and transportation and that we denote as "power-freshwater system". A general diagram of this system is depicted in Fig. 1. This requires a detailed characterization of the freshwater production and transportation system, which is provided below.
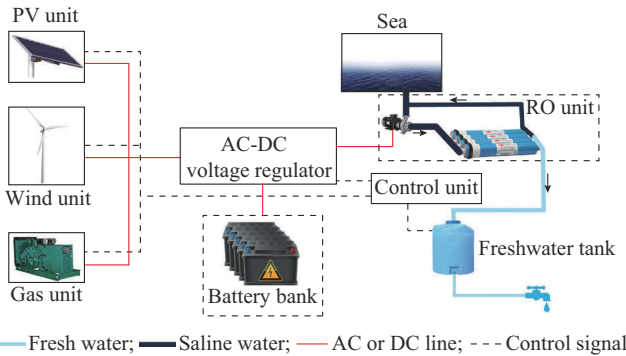


Fig. 1. Diagram of power-freshwater system.

### A. Objective Function

The objective considered is to minimize the power system operation cost one day in advance considering hourly steps. We note that the operation cost of producing and transporting freshwater is the amount of electrical energy consumed by pumps and desalination plants. This is translated in the objective function below:

$$\min_{\Psi_P \cup \Psi_W} \sum_{t=1}^{T} \left( \sum_u \alpha_u^E P_u^E(t) + \sum_u \alpha_u^F w_u(t) + \sum_u \alpha_u^{SU} y_u(t) + \right.$$
$$\sum_u \alpha_u^{SD} x_u(t) + \sum_k \alpha_k^W P_k^W(t) + \sum_v \alpha_v^{PV} P_v^{PV}(t) +$$
$$\left. \sum_z \alpha_z^{LS} P_z^{LS}(t) + \sum_m \alpha_m^{UW} d_m^{UW}(t) \right) \qquad (1)$$

The objective function (1) is composed of eight terms: ① $\sum_t \sum_u \alpha_u^E P_u^E(t)$ is the generation cost of all gas units, ② $\sum_t \sum_u \alpha_u^F w_u(t)$ is the no-load cost of all gas units, ③ $\sum_t \sum_u \alpha_u^{SU} y_u(t)$ is the start-up cost of all gas units, ④ $\sum_t \sum_u \alpha_u^{SD} x_u(t)$ is the shut-down cost of all gas units, ⑤ $\sum_t \sum_k \alpha_k^W P_k^W(t)$ is the generation cost of all wind units, ⑥ $\sum_t \sum_v \alpha_v^{PV} P_v^{PV}(t)$ is the generation cost of all PV units, ⑦ $\sum_t \sum_z \alpha_z^{LS} P_z^{LS}(t)$ is the unserved-energy cost of all electric demands, and ⑧ $\sum_t \sum_m \alpha_m^{UW} d_m^{UW}(t)$ is the unserved-freshwater cost of all freshwater demands.

### B. Power System Constraints

The specific constraints of the power system are stated as:

$$P_k^W(t) \le \mu_{W_k}(t) - \phi^{-1}(1-\epsilon)\sigma_{W_k}(t) \quad \forall k, \forall t \qquad (2)$$

$$P_v^{PV}(t) \le \mu_{PV_v}(t) - \phi^{-1}(1-\epsilon)\sigma_{PV_v}(t) \quad \forall v, \forall t \qquad (3)$$

$$E_b^B(t) = E_b^B(t-1) + \eta_b^C P_b^{Ch}(t) - \frac{1}{\eta_b^D} P_b^{Dis}(t) \quad \forall b, \forall t \qquad (4)$$

$$0 \le P_b^{Ch}(t) \le P_b^{Ch,\,max} \quad \forall b, \forall t \qquad (5)$$

$$0 \le P_b^{Dis}(t) \le P_b^{Dis,\,max} \quad \forall b, \forall t \qquad (6)$$

$$E_b^{min} \le E_b^B(t) \le E_b^{max} \quad \forall b, \forall t \qquad (7)$$

$$E_b^B(T) \ge E_b^B(0) \quad \forall b \qquad (8)$$

$$w_u(t) - w_u(t-1) = y_u(t) - x_u(t) \quad \forall u, \forall t \qquad (9)$$

$$y_u(t) + x_u(t) \le 1 \quad \forall u, \forall t \qquad (10)$$

$$\begin{cases} w_u(t) \in \{0,1\} \\ y_u(t) \in \{0,1\} \quad \forall u, \forall t \\ x_u(t) \in \{0,1\} \end{cases} \qquad (11)$$

$$P_u^{E,\,min} w_u(t) \le P_u^E(t) \le \bar{P}_u^E(t) \quad \forall u, \forall t \qquad (12)$$

$$\bar{P}_u^E(t) \le P_u^{E,\,max}(w_u(t) - x_u(t+1)) + \phi_u^{SD} x_u(t+1) \quad \forall u, \forall t \qquad (13)$$

$$\bar{P}_u^E(t) \le P_u^E(t-1) + \phi_u^U w_u(t-1) + \phi_u^{SU} y_u(t) \quad \forall u, \forall t \qquad (14)$$

$$P_u^E(t-1) - P_u^E(t) \le \phi_u^D w_u(t) + \phi_u^{SD} x_u(t) \quad \forall u, \forall t \qquad (15)$$

$$\sum_{u \in \Omega_n^U} P_u^E(t) + \sum_{k \in \Omega_n^K} P_k^W(t) + \sum_{v \in \Omega_n^V} P_v^{PV}(t) + \sum_{b \in \Omega_n^B} P_b^{Dis}(t) +$$
$$\sum_{\ell | r(\ell)=n} f_\ell^E(t) - \sum_{\ell | s(\ell)=n} f_\ell^E(t) = \sum_{b \in \Omega_n^B} P_b^{Ch}(t) + \sum_{s \in \Omega_n^S} P_s^{WP}(t) +$$
$$\sum_{z \in \Omega_n^Z} (P_z^{ZE}(t) - P_z^{LS}(t)) \quad \forall n, \forall t \qquad (16)$$

$$f_\ell^E(t) = K_\ell(\theta_{s(\ell)}(t) - \theta_{r(\ell)}(t)) \quad \forall \ell, \forall t \qquad (17)$$

$$-F_\ell^{max} \le f_\ell^E(t) \le F_\ell^{max} \quad \forall \ell, \forall t \qquad (18)$$

$$\sum_{u \in \chi_r^U} (\bar{P}_u^E(t) - P_u^E(t)) \ge R_r(t) \quad \forall r, \forall t \qquad (19)$$

$$0 \le P_z^{LS}(t) \le P_z^{ZE}(t) \quad \forall z, \forall t \qquad (20)$$

$$\begin{cases} w_u(t) \in \mathcal{A}_u \\ y_u(t) \in \mathcal{A}_u \quad \forall u, \forall t \\ x_u(t) \in \mathcal{A}_u \end{cases} \quad (21)$$

Constraints (2) and (3) are the deterministic chance constraints for uncertain wind and PV power outputs, respectively. Constraint (4) calculates the state-of-charge (SOC) of batteries at the end of hour $t$. Constraints (5)-(7) impose bounds on the charging rate, discharging rate, and SOC of batteries, respectively, during all hours. Constraint (8) ensures the availability of sufficient energy in batteries for next day [14], [15]. We note that the model for batteries is based on linear constraints (4)-(8). Such approximation is valid because the objective function (1) includes non-negative linear operation costs for gas units, and the power output of gas units is bounded by (12) [16]. Constraints (9)-(11) impose the on/off logic constraints for gas units [17]. Constraint (12) enforces gas units to operate within their maximum and minimum power limits. Constraints (13) and (14) express the maximum power output of gas units. Constraint (15) expresses the ramp-down limit of gas units [18]. Constraint (16) enforces the supply-demand balance in each node of the power system. Constraints (17) and (18) calculate the power flow and enforce the flow limit through each line, respectively. Constraint (19) imposes a spinning reserve requirement in each region $r$ [19], [20]. Constraint (20) bounds the unserved energy by the corresponding electrical load. Finally, constraint (21) imposes the minimum-up time and minimum-down time requirements for each gas unit [18].

### C. Freshwater System Constraints

The specific constraints regarding the production and transportation of freshwater are stated below. The freshwater system comprises desalination plants, pumps, pipelines, tanks, and demands [6], [11]. These constraints are nonlinear due to pump operation and pipeline loss equations.

As it is customary in short-term studies, we assume that the pump scheduling states are known and freshwater flows in single direction through pumps. These assumptions are justified in [12], [21], [22]. The constraints are given as:

$$V_q^{\mathrm{W}}(t) = V_q^{\mathrm{W}}(t-1) + f_q^{\mathrm{C}}(t) - f_q^{\mathrm{D}}(t) \quad \forall q, \forall t \quad (22)$$

$$V_q^{\mathrm{W}}(T) = V_q^{\mathrm{W}}(0) \quad \forall q \quad (23)$$

$$V_q^{\mathrm{W,min}} \le V_q^{\mathrm{W}}(t) \le V_q^{\mathrm{W,max}} \quad \forall q, \forall t \quad (24)$$

$$0 \le f_q^{\mathrm{C}}(t) \le f_q^{\mathrm{C,max}} \quad \forall q, \forall t \quad (25)$$

$$0 \le f_q^{\mathrm{D}}(t) \le f_q^{\mathrm{D,max}} \quad \forall q, \forall t \quad (26)$$

$$\sum_{c \in \Omega_i^{\mathrm{C}}} g_c^{\mathrm{W}}(t) + \sum_{j|r(j)=i} f_j^{\mathrm{W}}(t) - \sum_{j|s(j)=i} f_j^{\mathrm{W}}(t) + \sum_{q \in \Omega_i^{\mathrm{Q}}} f_q^{\mathrm{D}}(t) =$$
$$\sum_{m \in \Omega_i^{\mathrm{M}}} (d_m^{\mathrm{W}}(t) - d_m^{\mathrm{UW}}(t)) + \sum_{q \in \Omega_i^{\mathrm{Q}}} f_q^{\mathrm{C}}(t) \quad \forall i, \forall t \quad (27)$$

$$(h_{s(j)}^{\mathrm{P}}(t) + h_{s(j)}^{\mathrm{Z}}) = h_j^{\mathrm{F}}(t) + (h_{r(j)}^{\mathrm{P}}(t) + h_{r(j)}^{\mathrm{Z}}) \quad \forall t, \forall j/j\{s\} \quad (28)$$

$$(h_{s(j)}^{\mathrm{P}}(t) + h_{s(j)}^{\mathrm{Z}}) + h_{j\{s\}}(t) = h_j^{\mathrm{F}}(t) + (h_{r(j)}^{\mathrm{P}}(t) + h_{r(j)}^{\mathrm{Z}}) \quad \forall t, \forall j\{s\} \quad (29)$$

$$h_i^{\mathrm{P,min}} \le h_i^{\mathrm{P}}(t) \le h_i^{\mathrm{P,max}} \quad \forall i, \forall t \quad (30)$$

$$0 \le d_m^{\mathrm{UW}}(t) \le d_m^{\mathrm{W}}(t) \quad \forall m, \forall t \quad (31)$$

$$0 \le f_j^{\mathrm{W}}(t) \le f_j^{\mathrm{W,max}} \quad \forall j, \forall t \quad (32)$$

$$h_j^{\mathrm{F}}(t) = R_j (f_j^{\mathrm{W}}(t))^2 \quad \forall j, \forall t \quad (33)$$

$$h_s(t) = \mu_s (\omega_s^{\mathrm{WP}}(t))^2 - \beta_s (f_{j\{s\}}^{\mathrm{W}}(t))^2 \quad \forall t, \forall s \quad (34)$$

$$P_s^{\mathrm{WP}}(t) = \frac{\lambda}{\eta_s} f_{j\{s\}}^{\mathrm{W}}(t) h_s(t) \quad \forall s, \forall t \quad (35)$$

$$g_c^{\mathrm{W}}(t) \in \mathcal{D}_c \quad \forall c, \forall t \quad (36)$$

$$0 \le P_s^{\mathrm{WP}}(t) \le P_s^{\mathrm{WP,max}} \quad \forall s, \forall t \quad (37)$$

$$0 \le g_c^{\mathrm{W}}(t) \le g_c^{\mathrm{W,max}} \quad \forall c, \forall t \quad (38)$$

Constraint (22) calculates the freshwater levels in freshwater tanks for each hour. At the beginning of the planning horizon, constraint (22) is $V_q^{\mathrm{W}}(1) = V_q^{\mathrm{W}}(0) + f_q^{\mathrm{C}}(1) - f_q^{\mathrm{D}}(1), \forall q$, where $V_q^{\mathrm{W}}(0)$ is the freshwater level of tank $q$ at the end of $t=0$. Constraint (23) enforces the freshwater levels of freshwater tanks at the end of the planning horizon to be equal to their respective levels at the beginning of the planning horizon. This policy ensures that enough freshwater is available at the beginning of the next day. Constraints (24)-(26) limit freshwater levels, inflow levels, and outflow levels of freshwater tanks, respectively. Constraint (27) represents the supply-demand balance at each node of the freshwater system. Constraints (28) and (29) represent the nodal head pressures for all pipelines and pumps in the freshwater system, respectively [23]-[25]. Constraints (30)-(32) limit the hourly nodal head pressures, unserved freshwater, and pipeline flows, respectively. Constraint (33) is the Hazen-Williams equation for friction losses in pipelines [25]. Constraints (34) and (35) represent the hourly pump operation [6], [26], [27]. Constraint (36) represents the freshwater production of desalination plants [26], [28]. Constraints (37) and (38) enforce limits on the energy usage of pumps and on freshwater production from desalination plants, respectively.

### D. Optimization Variables

The optimization variables of the daily scheduling problem (1)-(38) regarding power and freshwater are given in (39) and (40), respectively:

$$\Psi_P = \{\theta_n(t), f_\ell^{\mathrm{E}}(t), P_u^{\mathrm{E}}(t), \bar{P}_u^{\mathrm{E}}(t), P_k^{\mathrm{W}}(t), P_v^{\mathrm{PV}}(t), P_z^{\mathrm{LS}}(t),$$
$$E_b^{\mathrm{B}}(t), P_b^{\mathrm{Ch}}(t), P_b^{\mathrm{Dis}}(t), w_u(t), y_u(t), x_u(t)\} \quad (39)$$

$$\Psi_W = \{g_c^{\mathrm{W}}(t), d_m^{\mathrm{UW}}(t), V_q^{\mathrm{W}}(t), f_q^{\mathrm{C}}(t), f_q^{\mathrm{D}}(t), f_j^{\mathrm{W}}(t),$$
$$P_s^{\mathrm{WP}}(t), h_j^{\mathrm{F}}(t), h_i^{\mathrm{P}}(t), h_s(t), \omega_s^{\mathrm{WP}}(t)\} \quad (40)$$

### E. Linearization

We note that the daily scheduling model of power-freshwater system above is a mixed-integer nonlinear problem due to freshwater constraints (33)-(36). We linearize these constraints using standard piecewise linearization techniques for functions of one and two variables, as described in [29]. The detailed description of piecewise linearizations associated with univariate functions is provided in Appendix A Section A, while that associated with bivariate functions is provided in Appendix A Section B. The resulting problem is an MILP problem that is solved using a state-of-the-art branch-and-cut solver [30].

### III. CASE STUDIES

We consider three case studies based on the IEEE 118-bus system linked to two 13-node freshwater systems, as shown in Fig. 2 [5], [31]. The first case represents the operation of a thermal-dominated power-freshwater system, whereas the second case represents the operation of a renewable-dominated power-freshwater system, and the last case represents the operation of a fully renewable power-freshwater system. The details of the three cases are given as follows.
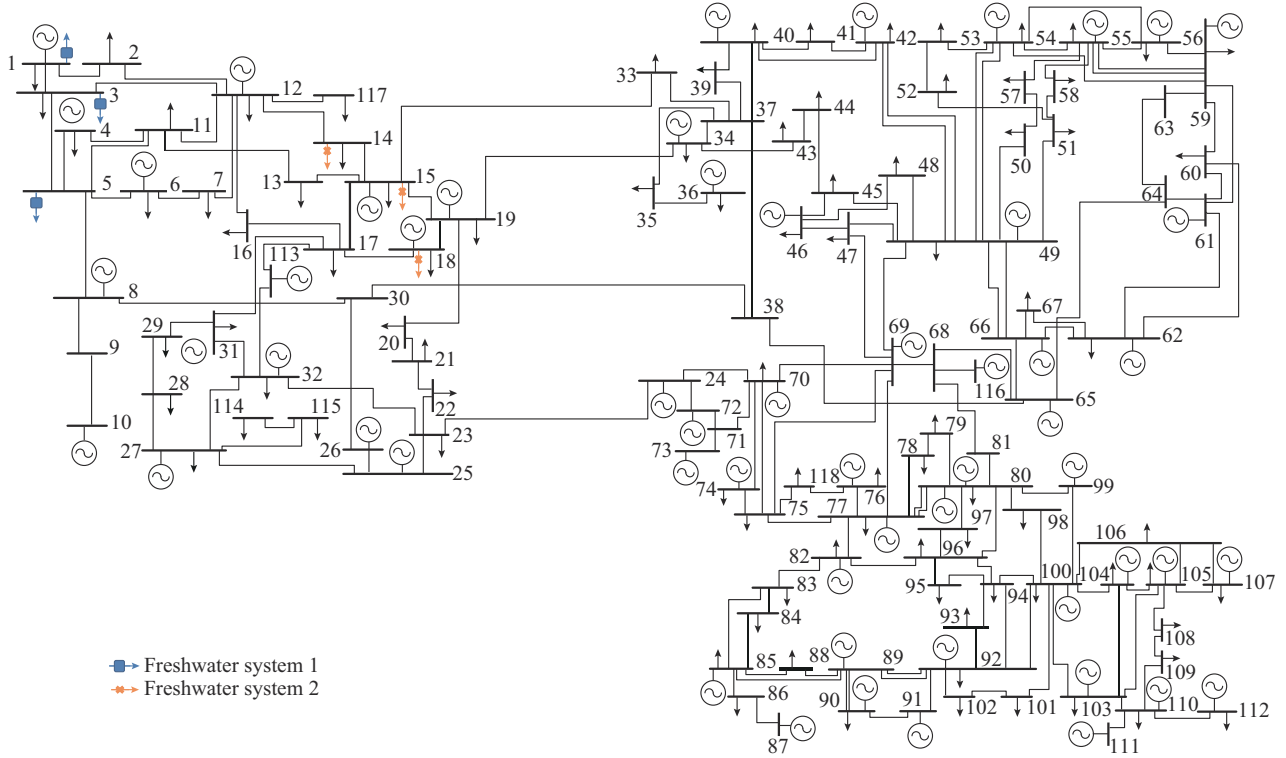


Fig. 2.   Schematic of IEEE 118-bus system.

1) Case 1: 10 PV units with a capacity of 5 GW, 17 wind units with a capacity of 5.1 GW, and 54 gas units with a capacity of 12 GW constitute the generation mix. Hence, the percentage of the renewable (PV+wind) capacity to the total capacity in this case is equal to 45%. No batteries are considered in this case.

2) Case 2: to create a renewable-dominated system, we decrease the capacity of the gas units to 4.41 GW, while increasing the capacity of PV unit to 14.5 GW. The capacity of wind units is kept at the same level. The renewable penetration level in this case is equal to 81%. Further, 27 batteries are incorporated in the power system. The power and energy capacities of all batteries are 10.8 GW and 108 GWh, respectively.

3) Case 3: to create a fully renewable power system, we suppress gas units, and increase the PV capacity to 20.0 GW. The capacity of wind unit is kept at the same level. Additionally, we increase the number of batteries to 33. The power and energy capacities of all batteries are 13.2 GW and 132 GWh, respectively.

The total capacity of freshwater tank remains unchanged across the three cases above.

We note that we do not solve an expansion planning problem here, but use reasonable power capacity values for each of the three cases described above.

Moreover, investing in freshwater tanks is generally cheaper than installing electrical batteries and thus, from an invest-

ment point of view, the rule "invest in water tanks as long as an economic incentive exists" is applied. However, the freshwater tanks solely impact the demand pertaining to freshwater, not other demands, and thus electrical batteries might be beneficial regarding these other demands. Nevertheless, both impacts are related through the power system and analyzing the interaction of these two impacts is the purpose of this paper, which focuses on operation.

We report the operation outcomes of the power-freshwater system in these three cases with particular attention to the tradeoff of storing freshwater in tanks versus storing electricity in batteries.

#### A. Data

The considered IEEE power system comprises 118 buses and 186 lines. It includes 91 demands not associated with the two freshwater systems. As shown in Fig. 2, the two freshwater systems 1 and 2 are incorporated into the power system as six freshwater system loads. Each battery has a power capacity of 400 MW and an energy capacity of 4000 MWh. The charging efficiency is assumed to be 93% and discharging efficiency is assumed to be 91% [32]. The required power system reserves in the three reserve zones are assumed to be equal to 10% of the electric demand.

The first freshwater system [6], [33], as shown in Fig. 3, comprises 13 nodes ($I_1$-$I_{13}$) and 12 pipelines ($J_1$-$J_{12}$) and includes one desalination plant ($C_1$), two pumps, two freshwa-

ter tanks ($Q_1$ and $Q_2$), and three freshwater demands ($M_1$-$M_3$). We note that this freshwater system includes several junction (connection) points between pipelines. Valves are commonly installed in these points in order to maintain both the pressure and flow levels of freshwater within pipeline limits, ensuring that they remain at safe levels. Besides, they are used to isolate portions of pipelines for maintenance purposes, and to avoid undesirable backflow of freshwater [34], [35]. Each desalination plant comprises a pump and membranes [28]. Unlike pumps, membranes do not consume electricity. Three centrifugal pumps (two for freshwater transportation and one for freshwater production) are considered. Each pump rating is equal to 60 MW [36], [37]. The desalination plant is connected to the power system at node 1, the pump in the first pipeline at node 3, and the third pump at node 5.
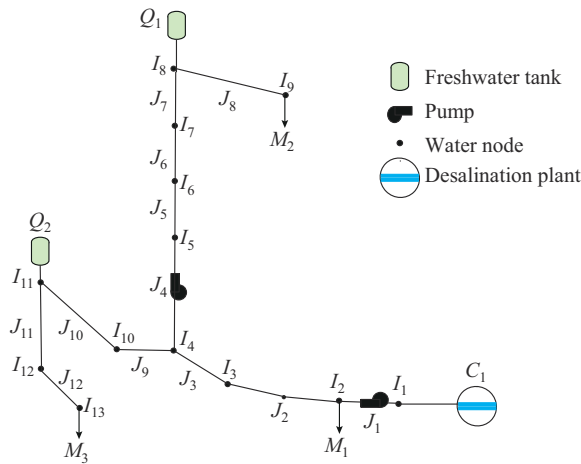


Fig. 3. Schematic of 13-node freshwater system.

An additional identical freshwater system 2, connected at different nodes, is also considered. The second desalination plant is connected to the power system at node 14, the pump in the first pipeline at node 15, and the third pump at node 18.

Freshwater node data, pipeline data, freshwater storage tank data, and freshwater demand data are provided in [38]. The total electric demand from the two freshwater systems is approximately equal to 12% of the total electric demand.

A macOS Catalina-based laptop with an 8-Core Intel Core i9 processor clocking at 2.30 GHz and 32 GB of RAM is used for the simulations reported below.

*B. Results*

The linearized version of the day-ahead power-freshwater scheduling problem (1)‑(38) is solved using GUROBI [30] under GAMS [39] for the three cases.

Table I provides the total cost and computation time for Cases 1-3. We note that the time is commensurate with an operation time frame.

The solution outcomes obtained using the proposed linearization is accurate enough (within an 5% error bound) and can be asymptotically improved by increasing linearization segments (one variable) and linearization triangles (two variables).

TABLE I
TOTAL COST AND COMPUTATION TIME

| Case | Cost ($) | Computation time (min) |
|---|---|---|
| Case 1 | 1927388 | 72.58 |
| Case 2 | 1312510 | 20.40 |
| Case 3 | 723684 | 58.72 |

From the simulations carried out, we can conclude that the resulting MILP model is robust and numerically stable.

The power outputs of renewable units at the different penetration levels are depicted in Fig. 4. Specifically, this figure shows the total power outputs of PV and wind units for Cases 1-3. It also shows the curtailed power of renewable units in Cases 2 and 3. We note that the curtailment power in Case 1 is zero. The total curtailment energy is equal to 3.142 GWh in Case 2, and increases by 63% (5.130 GWh) in Case 3. This increase in curtailed energy is due to the physical limits of batteries. Particularly, batteries are operating at their charging limits during peak hours 11-13.
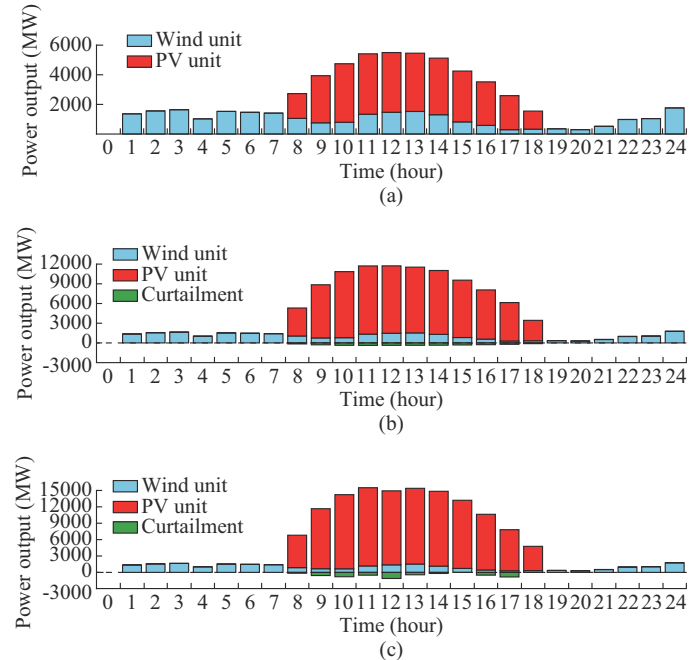


Fig. 4. Power outputs of renewable units. (a) Case 1. (b) Case 2. (c) Case 3.

We examine below the results obtained in Cases 1-3 considered and highlight important differences between them.

*1) Desalination Plant Operation*

Figure 5 shows freshwater demand and production in Cases 1-3. The upper subplot depicts the hourly freshwater demand, and the lower subplot presents the total freshwater output of all desalination plants per hour for the three cases.

In Case 1, the total freshwater output of all desalination plants (lower subplot) is constant at 118684 m³/h during hours 1-7; then, the output reaches the peak at 198477 m³/h during hour 11, decreases to 118684 m³/h during hour 15, and continues at the same rate for the remaining planning horizon. However, in Case 2, the total output of desalination

plant is 120407 m³/h during hours 1-7; then, the output reaches the peak at 197025 m³/h during hour 11, decreases to 118684 m³/h during hour 19, and finally continues at the same rate for the remaining operation horizon.
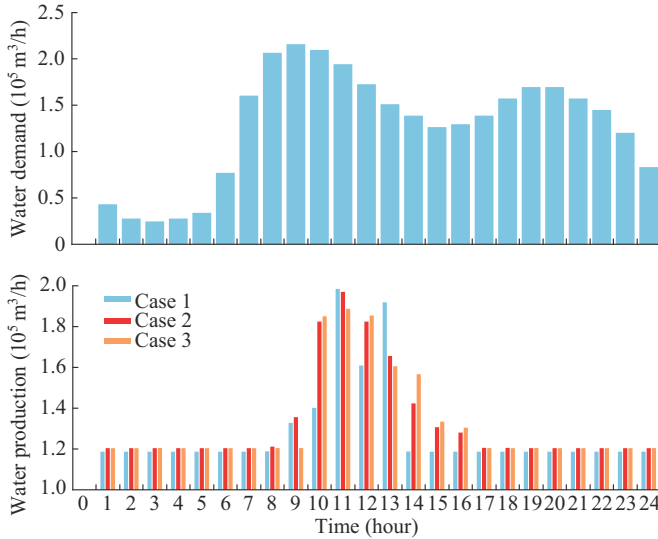


Fig. 5.　Freshwater demand and production.

From this figure, we observe that the total output of the desalination plant is closer to the PV plant operation in Case 2. This is because the PV unit starts producing nonzero power during hour 8, gradually increases its output to its peak during hour 11, and then gradually decreases to zero again during hour 19. Consequently, the desalination plant operation follows the PV unit operation to a greater extent as the renewable penetration increases. Moreover, the peak production of the desalination plants in Case 3 is lower than that in Case 2, and that in Case 2 is lower than that in Case 1. In particular, the peak of desalination plants is about 1% lower in Case 2 than that in Case 1, and 4% lower in Case 3 than in Case 2. Increasing the penetration level of the renewable units in this case reduces the peak output of the desalination plants.

*2) Freshwater Tank Operation*

Figure 6 shows the freshwater volume in all freshwater tanks in Cases 1-3. It is relevant to note that freshwater tanks are more extensively used if the renewable capacity is higher. Particularly, in Case 2, the total freshwater content in tanks decreases from 728162 to 396763 m³ during hours 6-12. However, in Case 1, it decreases from 717822 to 428677 m³ during the same hours. Consequently, freshwater tanks discharge additional 42254 m³ (increase of 14.61%) in Case 2 relative to Case 1. Similarly, freshwater tank discharging volume increases by 31.70% in Case 3 relative to Case 2. Therefore, in this case with higher renewable capacity, the total tank discharging volume also increases.

*3) Electrical Battery Operation*

In this part, we consider Cases 2 and 3 (no batteries in Case 1). Figure 7 depicts the total stored energy in all batteries per hour for Cases 2 and 3. It is important to note that the initial value of the energy content of the batteries is selected to be 65000 MWh to ensure a power system opera-
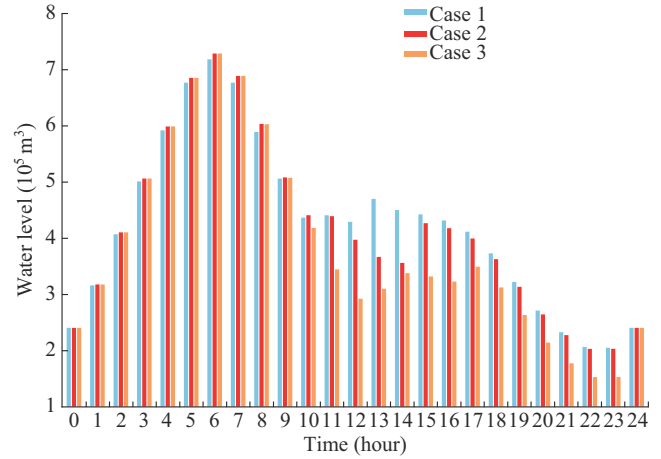
tion with no unserved energy.
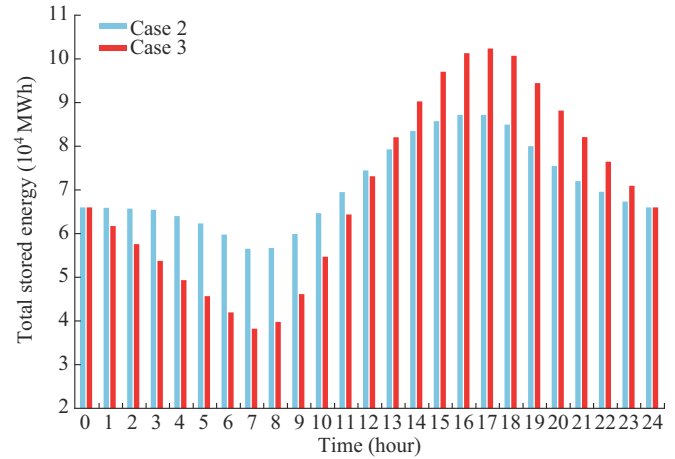


Fig. 6.　Freshwater volume in freshwater tanks.



Fig. 7.　Total stored energy in all batteries.

We observe that batteries charge/discharge higher levels of energy as the renewable penetration level increases. As expected, increasing renewable capacity and reducing thermal capacity necessitate high deployment of batteries.

On the one hand, batteries discharge 9.471 GWh of energy during hours 0-7 in Case 2 and 27.764 GWh during the same hours in Case 3. Hence, the discharging energy of the batteries is lower by 65.89% in Case 2 as compared with Case 3. On the other hand, batteries charge 60.935 GWh of energy during hours 8-18 in Case 3 but 28.239 GWh during the same hour in Case 2. Therefore, the charging energy of batteries is lower by 53.66% in Case 2 as compared with Case 3. From the above, we observe that the utilization of batteries during an operation cycle increases as the renewable capacity increases.

Besides, the operation of batteries is closely related to the operation of the renewable units. Specifically, the batteries discharge energy during hours 0-7 when the PV units are offline, and store energy during hours 8-18 when the PV units are online. Finally, they discharge energy at the end of the planning horizon when the PV units are offline. The operation pattern of the batteries follows the operation pattern of the PV units instead of that of the wind units owing to the

higher capacity of PV units in the case studies analyzed.

Additionally, batteries are highly utilized during an operation cycle. For example, in Case 3, the minimum level of stored energy is 38235 MWh, whereas its maximum level is 102370 MWh. That is, the ratio of the peak level to the minimum level is about 2.68.

### 4) Electrical Batteries Versus Freshwater Tanks

We assess the performance of freshwater tanks and batteries in terms of their usage levels. Regarding batteries, we calculate the incremental change of the total energy content for all cases, as shown in Fig. 8. To this end, we calculate the absolute value of the relative increment of the energy content for each two consecutive hours starting at hour 0 and ending at hour 23. We use the same technique for calculating the incremental change of the freshwater level in freshwater tanks.
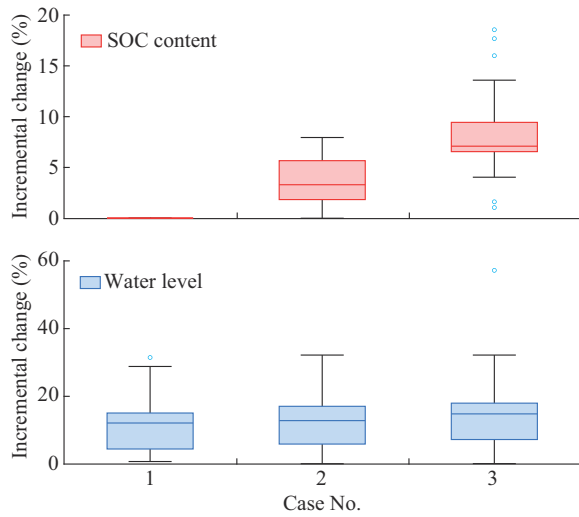


Fig. 8.    Incremental changes in freshwater tanks and batteries.

Figure 8 shows the incremental changes in all freshwater tanks and batteries for Cases 1-3. The upper subplot corresponds to incremental changes of the total electrical energy stored in all batteries, whereas the lower subplot corresponds to the changes of the freshwater content in all freshwater tanks.

In Case 1, we note that the freshwater tanks are intensively charging/discharging freshwater. The median of the incremental changes of the freshwater tanks is 12.12%. The corresponding medians of Cases 2 and 3 are 12.83% and 14.2%, respectively. The lower and upper quartiles of Case 1 are 4.45% and 15.07%, respectively. Those values in Case 2 are 5.90% and 17.06%, respectively, whereas those in Case 3 are 7.24% and 17.99%, respectively. We observe that all of the above statistical values in Case 2 are larger than those in Case 1, and those in Case 3 are larger than those in Case 2. Hence, the usage extent of freshwater tanks increase as the renewable penetration increases.

Overall, the incremental changes of freshwater tanks are larger than those of batteries. In particular, the medians of the incremental changes of the SOC content in Cases 2 and 3 are 3.30% and 7.09%, respectively. Comparing these two

medians (3.30% and 7.09%) associated with incremental changes of batteries with those of freshwater tanks, we observe that those medians of freshwater tanks are about 4 and 2 times higher than those of batteries in Cases 2 and 3, respectively. As expected, the usage extent of the freshwater tanks is higher than that of the batteries due to their higher efficiency.

### 5) Increasing Battery Capacity Versus Increasing Freshwater Tank Capacity

We analyze below the impact on production cost (objective function) of limited capacity of freshwater tanks versus limited storage capacity in batteries.

To this end, we systematically reduce capacity of freshwater tank until constraint (24) becomes binding during some hours while not binding during most hours. Similarly, we gradually reduce battery capacity until constraint (7) becomes binding during some hours. Particularly, we consider Case 3 and reduce the total freshwater tank capacity from 800000 to 769000 $m^3$, and reduce the total storage capacity of batteries from 132 GWh to 125.8 GWh. This way, tank and battery bounds, i.e., (24) and (7), respectively, become binding during some hours.

Figure 9 provides the dual variables of (24) for a specific freshwater tank and (7) for a specific battery, throughout the 24 hours of the scheduling horizon, in absolute value. These dual variables are always non-positive. That is, increasing the upper bound will decrease the optimal value of the objective function. The upper subplot of Fig. 9 provides the dual variables of constraint (24) in $/m^3$. We observe that this constraint becomes binding during hours 15-17. The actual values of the corresponding dual variables are commensurate with the cost of producing energy, which is about 5 $/MWh (Case 3 is a fully renewable case). The lower subplot of Fig. 9 provides the dual variables of constraint (7) in $/MWh. We observe that this constraint becomes binding during hours 14, 16, and 17. The actual values of the corresponding dual variables are also commensurate with the cost of producing energy.
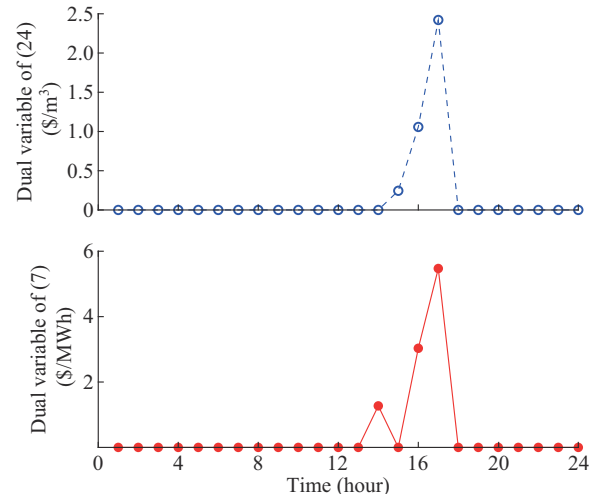


Fig. 9.    Shadow prices of capacity constraints for a specific freshwater tank and a specific battery.

We observe that marginally increasing the capacity of freshwater tanks has less impact on the objective function (production cost) than marginally increasing the storage capacity in batteries. Expansion decisions, though, need to be made considering the investment cost of expanding tank capacity versus the investment cost of expanding battery energy capacity. This is, though, beyond the scope of this paper.

We note that the purpose of this part is to analyze the impact of having storage capacity (of both batteries and freshwater tanks) just "at the limit". That is, having a storage capacity that most of the time is not binding, but binding is during some hours. In such circumstances, we analyze the cost consequences of these binding constraints (that occur during few hours), and find that binding battery capacity has higher cost impact than binding tank capacity.

*6) Decreasing Battery Capacity Versus Decreasing Freshwater Tank Capacity*

We examine below the impacts of decreasing the battery/ tank capacity on the total operation cost.

Regarding Case 1, if we reduce the tank capacity by 20%, the operation cost would increase by 0.02%. This value is close to the solver tolerance, which means that the impact is negligible in this case.

Regarding Case 2, if we reduce the tank capacity by 20%, the operation cost increases by 0.18%, and if we reduce the battery capacity by 20%, it increases by 10.43%. In the case of reducing both tank and battery capacities by 20%, the total cost increases by 10.60%. We note that these cost increments add linearly.

Regarding Case 3, if we reduce the tank capacity by 20%, the operation cost increases by 0.01%, and if we reduce the battery capacity by 20%, the power demand needs to be curtailed. In the case of reducing both tank and battery capacities by 20%, the power demand needs to be curtailed as well.

As expected, a decrement in battery capacity has a larger impact on operation cost than the same decrement in tank capacity. We also note that no unserved water occurs, but power demand needs to be curtailed.

## IV. Conclusion

In this paper, we consider the operation of three power systems that have different renewable configurations: moderate renewable penetration, high renewable penetration, and full renewable penetration. Each of these systems includes a large power demand due to freshwater production and transportation. In the three configurations, freshwater can be stored in water tanks in bulk quantities to shift the electric demand, and for the last two configurations, electrical batteries are available to facilitate renewable integration and system operation. Extensive numerical simulation allows us to have the following conclusions.

1) The higher the renewable penetration, the higher the usage of batteries and the higher the usage of freshwater tanks.

2) As the renewable penetration increases, the peak electric demand and the peak water demand decrease because of storage (of freshwater and electricity) usage.

3) The per-hour change of freshwater content in tanks is larger than the per-hour change in the energy content of batteries. This is because the overall efficiency of freshwater tanks is higher than that of batteries.

4) A marginal increase in battery capacity generally has a larger impact on the production cost than a marginal increase in freshwater-tank capacity.

5) Freshwater tanks solely impact freshwater power demand, but electrical batteries impact all power demands. It is important to note that both impacts are related through the power system operation.

On the other hand, considering the three renewable configurations, the proposed MILP model is adequately accurate and computationally robust, and it can be solved in a reasonable amount of time.

## Appendix A

### A. Piecewise Linearization

Regarding the piecewise linearization, we use $N$ breakpoints $(x_1, x_2, ..., x_N)$ and evaluate the nonlinear function at these breakpoints $(f(x_1), f(x_2), ..., f(x_N))$. We then approximate the function value at point $\tilde{x}$ using a convex combination of the function values at the vertices of the line segment $[x_r, x_{(r+1)}]$ containing point $\tilde{x}$.

### B. Triangular Linearization

The triangular linearization technique is an extension of the one-dimensional piecewise linearization technique [29]. In this linearization, we use $N$ breakpoints $(x_1, x_2, ..., x_N)$ for variable $x$ and $K$ breakpoints $(y_1, y_2, ..., y_K)$ for variable $y$. Then, we evaluate the function at each breakpoint $(f(x_r, y_v), \forall r, \forall v)$. Using these breakpoints, we obtain the rectangle $((x_r, y_v), (x_r, y_{v+1}), (x_{r+1}, y_v), (x_{r+1}, y_{v+1}))$, and its upper left and lower right triangles, as depicted in Fig. B1.
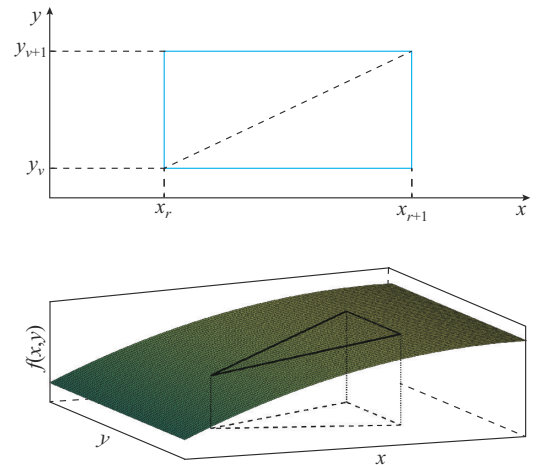


Fig. B1.   Triangle linearization.

In turn, we approximate the function value at point $(\tilde{x}, \tilde{y})$ using the convex combination of the function values at vertices of the upper left (or lower right) triangle containing point $(\tilde{x}, \tilde{y})$.

## References

[1] The Middle East. (2023, Aug.). Middle east increasingly reliant on desalination plants. [Online]. Available: https://www.thenationalnews.com

[2] Kuwait Finance House. (2023, Aug.). Kuwait annual report 2022. [Online]. Available: https://www. mew. gov. kw/media/2i1l4phf/final-water-book-2021-compressed.pdf

[3] ACWA Power. (2023, Aug.). ACWA power IWP project. [Online]. Available: https://www.acwapower.com

[4] L. A. Roald, "Optimization methods to manage uncertainty and risk in power systems operation," Ph. D. dissertation, ETH Zurich, Zurich, Switzerland, 2016.

[5] IEEE (2023, Aug.). IEEE 118 bus. [Online]. Available: https://labs.ece.uw.edu/pstca/pf118/pg tca118bus.htm

[6] K. Oikonomou and M. Parvania, "Optimal coordination of water distribution energy flexibility with power systems operation," *IEEE Transactions on Smart Grid*, vol. 10, no. 1, pp. 1101-1110, Jan. 2019.

[7] F. Moazeni and J. Khazaei, "Optimal design and operation of an islanded water-energy network including a combined electrodialysis-reverse osmosis desalination unit," *Renewable Energy*, vol. 167, pp. 395-408, Apr. 2021.

[8] P. Zhao, C. Gu, Z. Cao *et al*., "Water-energy nexus management for power systems," *IEEE Transactions on Power Systems*, vol. 36, no. 3, pp. 2542-2554, May 2021.

[9] L. Edmonds, M. Derby, M. Hill *et al*., "Coordinated operation of water and electricity distribution networks with variable renewable energy and distribution locational marginal pricing," *Renewable Energy*, vol. 177, pp. 1438-1450, Nov. 2021.

[10] H. Mehrjerdi, "Modeling and integration of water desalination units in thermal unit commitment considering energy and water storage," *Desalination*, vol. 483, p. 114411, Jun. 2020.

[11] Q. Li, S. Yu, A. S. Al-Sumaiti *et al*., "Micro water-energy nexus: optimal demand-side management and quasi-convex hull relaxation," *IEEE Transactions on Control of Network Systems*, vol. 6, no. 4, pp. 1313-1322, Dec. 2019.

[12] D. Li, C. Gao, T. Chen *et al*., "Day-ahead scheduling of integrated power and water system considering a refined model of power-to-gas," *IEEE Access*, vol. 10, pp. 88894-88904, Aug. 2022.

[13] M. Sun, X. Li, H. Tan *et al*., "Probabilistic optimal power-water flow analysis of integrated electricity-water system considering uncertainties and correlations," in *Proceedings of 2020 IEEE 4th Conference on Energy Internet and Energy System Integration (EI2)*, Wuhan, China, Oct. 2020, pp. 1349-1354.

[14] Y. Wen, C. Guo, H. Pandžić *et al*., "Enhanced security-constrained unit commitment with emerging utility-scale energy storage," *IEEE Transactions on Power Systems*, vol. 31, no. 1, pp. 652-662, Jan. 2016.

[15] H. Pandžić and V. Bobanac, "An accurate charging model of battery energy storage," *IEEE Transactions on Power Systems*, vol. 34, no. 2, pp. 1416-1426, Mar. 2019.

[16] K. Garifi, K. Baker, D. Christensen *et al*., "Convex relaxation of grid-connected energy storage system models with complementarity constraints in DC OPF," *IEEE Transactions on Smart Grid*, vol. 11, no. 5, pp. 4070-4079, Sept. 2020.

[17] A. J. Conejo and L. Baringo, *Power System Operations*. New York: Springer, 2018.

[18] J. M. Arroyo and A. J. Conejo, "Optimal response of a thermal unit to an electricity spot market," *IEEE Transactions on Power Systems*, vol. 15, no. 3, pp. 1098-1104, Aug. 2000.

[19] G. Morales-España, J. M. Latorre, and A. Ramos, "Tight and compact MILP formulation for the thermal unit commitment problem," *IEEE Transactions on Power Systems*, vol. 28, no. 4, pp. 4897-4908, Nov. 2013.

[20] B. Knueven, J. Ostrowski, and J. P. Watson, "On mixed-integer programming formulations for the unit commitment problem," *INFORMS Journal on Computing*, vol. 32, no. 4, pp. 857-876, Jun. 2020.

[21] A. S. Zamzam, E. Dall'Anese, C. Zhao *et al*., "Optimal water-power flow-problem: formulation and distributed optimal solution," *IEEE Transactions on Control of Network Systems*, vol. 6, no. 1, pp. 37-47, Mar. 2019.

[22] D. Fooladivanda and J. A. Taylor, "Energy-optimal pump scheduling and water flow," *IEEE Transactions on Control of Network Systems*, vol. 5, no. 3, pp. 1016-1026, Sept. 2018.

[23] A. L. Gerhart, J. I. Hochstein, and P. M. Gerhart, *Munson, Young and Okiishi's Fundamentals of Fluid Mechanics*. Hoboken: John Wiley & Sons, 2020.

[24] A. Akan, R. J. Houghtalen, and N. Hwang, *Fundamentals of Hydraulic Engineering Systems*. Upper Saddle River: Pearson, 2010.

[25] L. W. Mays, *Water Resources Engineering*. Hoboken: John Wiley & Sons, 2010.

[26] K. Oikonomou and M. Parvania, "Optimal coordinated operation of interdependent power and water distribution systems," *IEEE Transactions on Smart Grid*, vol. 11, no. 6, pp. 4784-4794, Nov. 2020.

[27] M. Majidi, L. Rodriguez-Garcia, M. Parvania *et al*., "Integration of small pumped storage hydropower units in water distribution system operation," in *Proceedings of 2020 IEEE PES General Meeting (PESGM)*, Montreal, Canada, Aug. 2020, pp. 1-5.

[28] M. Mulder and J. Mulder, *Basic Principles of Membrane Technology*. New Jersey: Springer Science & Business Media, 1996.

[29] C. D'Ambrosio, A. Lodi, and S. Martello, "Piecewise linear approximation of functions of two variables in MILP models," *Operations Research Letters*, vol. 38, no. 1, pp. 39-46, Jan. 2010.

[30] NEOS solver. (2021, Nov.). Gurobi. [Online]. Available: https://neos-server.org/neos/solvers/milp:Gurobi/GAMS.html

[31] Texas A&M University. (2023, Aug.). Texas A&M University electric grid datasets. [Online]. Available: https://electricgrids. engr. tamu. edu/electric-grid-test-cases/ieee-118-bus-system/

[32] B. Yang, Y. Makarov, J. Desteese *et al*., "On the use of energy storage technologies for regulation services in electric power systems with significant penetration of wind energy," in *Proceedings of 2008 5th International Conference on the European Electricity Market*, Lisbon, Portugal, May 2008, pp. 1-6.

[33] USMART. (2022, Mar.). 15 node test water distribution system. [Online]. Available: https://usmart.ece.utah.edu/datasets/

[34] A. Martin, K. Klamroth, J. Lang *et al*., *Mathematical Optimization of Water Networks*. New York: Springer, 2012.

[35] L. W. Mays, *Water Distribution System Handbook*. New York: McGraw-Hill Education, 2000.

[36] Hitachi. (2023, Aug.). Hitachi pumps. [Online]. Available: https://www. vhpc. com. ve/presentations/eng/5%20Pump% 20Presentation% 20-% 20March%202008.pdf

[37] Hitachi. (2023, Aug.). Pumps and systems. [Online]. Available: https:// www.pumpsandsystems.com/success-story-year-2009-finalists-hitachi

[38] MEW. (2023, Aug.). Kuwait annual report 2021. [Online]. Available: https://www.mew.gov.kw/en/about/statistics

[39] M. R. Bussieck and A. Meeraus, "General algebraic modeling system (GAMS)," in *Modeling Languages in Mathematical Optimization*. New York: Springer, 2004.

**Mubarak J. Almubarak** received the B.Sc. degree from Kuwait University, Safat, Kuwait, in 2018, and the M.S. degree from The Ohio State University, Columbus, USA, in 2020. He is currently working toward the Ph.D. degree at the Department of Electrical and Computer Engineering, The Ohio State University. His research interests include operation and planning of power systems and freshwater systems, and integration of renewable energy, as well as optimization theory and its applications.

**Antonio J. Conejo** received the M.S. degree from the Massachusetts Institute of Technology, Cambridge, USA, in 1987, and the Ph.D. degree from the Royal Institute of Technology, Stockholm, Sweden, in 1990. He is currently a Professor at the Department of Integrated Systems Engineering and the Department of Electrical and Computer Engineering, The Ohio State University, Columbus, USA. His research interests include control, operations, planning, economics and regulation of electric energy systems, as well as statistics and optimization theory and its applications.